POWER SPECTRUM OF THE COSMIC MICROWAVE BACKGROUND RADIATION FROM THE COSMIC BACKGROUND IMAGER

Timothy J. Pearson

Owens Valley Radio Observatory, California Institute of Technology, Pasadena, CA 91125, USA

tjp@astro.caltech.edu

for the CBI collaboration[1]

ABSTRACT

The Cosmic Background Imager (CBI) is an interferometer array designed to measure the power spectrum of fluctuations in the cosmic microwave background radiation. The CBI is located at an altitude of 5080 m in northern Chile. It consists of 13 0.9-m diameter antennas on a 6-m diameter tracking platform. Each antenna has a cooled, low-noise receiver operating in the 26–36 GHz band. Signals are cross-correlated in an analog correlator with 10 1-GHz bands. We describe the observations and data-analysis methods and present a determination of the microwave background intrinsic anisotropy spectrum over the range $l = 400$ to $l = 3500$.

1. Introduction

The cosmic microwave background (CMB) provides a direct view of physical processes in the early universe. In standard cosmological models, acoustic oscillations of the primordial plasma give rise to a harmonic series of peaks in the angular power spectrum of the CMB (e.g., Sunyaev & Zeldovich 1970; Bond & Efstathiou 1987). Measurements of the power spectrum can provide strong constraints on cosmological parameters (e.g., White et al. 1994), determine the nature and initial conditions of the fluctuations (Hu & White 1996), and provide fundamental tests of particle physics (Kamionkowski & Kosowsky 1999). A number of experiments have detected the first, second, and possibly the third acoustic peaks in the anisotropy spectrum (Miller et al. 1999; de Bernardis et al. 2000; Hanany et al. 2000; Netterfield et al. 2002; Halverson et al. 2002; Lee et al. 2001). Observations at high multipoles ($l \sim 500$–2000), where the physics is strongly affected by photon diffusion and the thickness of the last scattering region (Silk 1968), provide independent constraints on these fundamental parameters. At even higher multipoles ($l > 2000$), secondary effects such as the Sunyaev-Zel'dovich effect (Sunyaev & Zel'dovich 1972) are expected to dominate and hence offer the prospect of studying the formation of large-scale structure at recent times.

The Cosmic Background Imager (CBI) is an interferometer array designed to measure the power spectrum of fluctuations in the CMB (CMBR) for multipoles in the range $400 < l < 3500$. The CBI is located at an altitude of 5080 m in the Atacama Desert in northern Chile. Here we present a summary of some of the results from the CBI. Preliminary results were presented by Padin et al. (2001, hereafter Paper I). Paper II (Mason et al. 2002) presents our estimate of the power spectrum for $l \lesssim 3500$ from observations of three pairs of $45'$ (FWHM) deep fields made in our first observing season, 2000 January–December. Paper III (Pearson et al. 2002) presents complementary results from first-season observations of three pairs of fields each about $145' \times 165'$ (total ≈ 40 deg^2), using the mosaicing method. While these observations are less sensitive than those of Paper II at high l, they have higher resolution in l, and they have greater sensitivity at low l owing to the reduced cosmic variance. Further observations made in 2001, which are currently being analyzed, will increase the sensitivity and improve the resolution of our power spectrum estimate. The method we use for extracting power spectrum estimates from interferometry data is described by Myers et al. (2002, hereafter Paper IV). A full discussion of the implications for cosmology is the subject of two further papers (Sievers et al. 2002, hereafter Paper V; Bond et al. 2002, hereafter paper VI).

---

[1]John Cartwright, Alison Farmer, Russ Keeney, Brian Mason, Steve Miller, Steve Padin (*Project Scientist*), Tim Pearson, Tony Readhead (*Principal Investigator*), Walter Schaal, Martin Shepherd, Jonathan Sievers, Patricia Udomprasert, and John Yamasaki (California Institute of Technology); Dick Bond, Carlo Contaldi, Ue-Li Pen, Dmitri Pogosyan, and Simon Prunet (CITA); John Carlstrom, Nils Halverson, Erik Leitch, John Kovac, and Clem Pryke (University of Chicago); Bill Holzapfel (University of California, Berkeley); Pablo Altamirano, Leonardo Bronfman, Simon Casassus, and Jorge May (University of Chile); Angel Otarola (ESO); Marshall Joy (NASA Marshall Space Flight Center).

2. The Cosmic Background Imager

Measurement of the CMB power spectrum with interferometers has been discussed in several papers (e.g., Hobson, Lasenby, & Jones 1995; Maisinger, Hobson, & Lasenby 1997; White et al. 1999a,b; Hobson & Maisinger 2002), and details of the method that we have used are presented in Paper IV. The angular power spectrum of the CMB is conventionally expressed as $C_l = \langle |a_{lm}|^2 \rangle$, where a_{lm} are the coefficients in a spherical-harmonic expansion of the CMB temperature distribution. A single-baseline interferometer is sensitive to a range of multipoles $l \approx 2\pi u \pm \Delta l/2$ where u is the baseline length in wavelengths, and Δl is the FWHM of the visibility window function, which is determined by the size and illumination pattern of the antennas and is proportional to the square of the Fourier transform of the primary beam (antenna power pattern). For a circular Gaussian primary beam of FWHM a rad, $\Delta l = 4\sqrt{2}\ln 2/a$.

The CBI is a 13 element interferometer in which all 78 antenna pairs are cross-correlated (for a detailed description, see Padin et al. 2002). The 26–36 GHz band is split into ten channels each 1 GHz wide, which are correlated separately, giving a total of 780 complex visibility measurements in each integration. The antennas are mounted on a tracking platform which is rotated to track parallactic angle, so that each baseline keeps a constant orientation relative to the field of view. The 78 baselines range in length from 1.0 m to about 5.5 m, depending on the antenna configuration on the platform. The antennas respond to left circular polarization (LCP), although for part of the observations one antenna was configured for right circular polarization (RCP). Data from the 12 cross-polarized baselines will be used to place limits on CMB polarization. The Cassegrain antennas have a diameter of 0.90 m and a measured primary beam width $a = 45\farcm2 \times (31\,\mathrm{GHz}/\nu)$ at frequency ν, so that $\Delta l \approx 300$. The primary beam is quite close to a circular Gaussian, but we have adopted a more accurate model of the measured radial profile when making images and estimating the CMB power spectrum.

In observations of single fields (Paper I and Paper II), the resolution in l of the power spectrum is limited to $\Delta l \sim 300$, which is insufficient to resolve the expected structure in the spectrum. To improve the resolution, we make *mosaiced* observations in which we map an area of sky using several closely-spaced pointings (Paper III). This method is in widespread use for making images of extended regions with radio interferometers. We have mapped three separate fields in this way, using 42 pointings for each in a rectangular grid of 7 rows separated by $20'$ in declination and 6 columns separated by $1^{\mathrm{m}}20^{\mathrm{s}} \approx 20'$ in right ascension. This allows us to improve the resolution in l to $\Delta l \approx 100$.

Although the CBI antennas were designed to have low sidelobes and crosstalk (Padin et al. 2000), emission from the ground contaminates the data, especially on short baselines. The ground signal is stable on time-scales of many minutes, so if we observe two nearby fields under similar ground conditions, the difference of the visibilities of the two fields is unaffected by the ground. Differencing also eliminates any constant or slowly varying instrumental offsets. We observe a field (the *lead* field) for about 8 min and then switch to a reference field (*trail* field) at the same declination but 8 min later in right ascension for the next 8 min, and form the difference of corresponding 8.4 s integrations. The two fields are observed over the same range of azimuth and elevation, so they have nearly identical ground contributions. Between scans, we rotate the platform to change its orientation relative to the hour circle, thus improving the sampling of the (u, v) plane. This also reduces the effect of any residual ground contamination.

3. Results

Figure 1 shows mosaic images made from the entire dataset using natural weighting (see Paper III). In the 26–36 GHz band, the dominant confusing foreground is the emission from discrete radio galaxies and quasars, which we refer to as "point sources." The contribution of point sources to the visibilities must be estimated accurately in order to obtain a reliable estimate of the CMB power spectrum. A random distribution of point sources has a power spectrum $C_l = \mathrm{constant}$, while for the CMB C_l decreases rapidly with increasing l, so discrete sources dominate at high l. To remove most of the point-source contamination in our data, we measured the flux densities of a large number of known point sources using a dual-beam 31 GHz HEMT receiver with a beamwidth of $81''$ on the 40-meter telescope at the Owens Valley Radio Observatory (OVRO), and subtracted the detected sources from the visibility data. The effectiveness of the OVRO source subtraction can be seen by comparison of the "before" and "after" images in Figure 1. Most of the sources have been removed successfully, although there are of course residuals owing to incorrect measurements or source variability, and a few sources can be seen that were not detected at OVRO.

Our algorithm for the estimation of power spectra from mosaic visibility data is described in Paper IV. We model the power spectrum as flat in each of a set of contiguous bands, and estimate the power in each band by maximum likelihood.

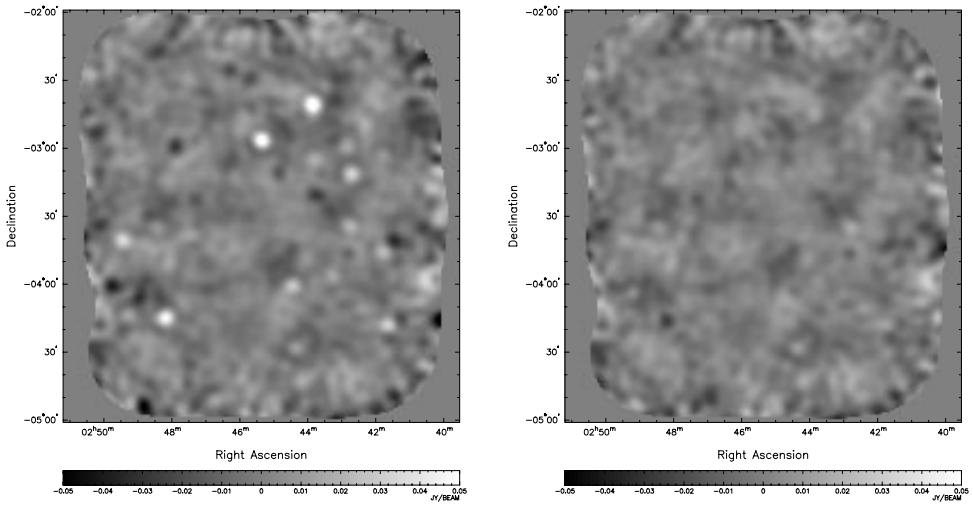

Fig. 1.— Images of the $02^{\rm h}$ mosaic field. *Left*: raw data; *right*: after subtraction of sources measured at OVRO. The images show the difference of the emission in the *lead* and *trail* fields. The coordinates are J2000. The right ascension scale applies to the *lead* field; add $8^{\rm m}$ to obtain the right ascension of objects in the *trail* field. The same gray-scale range has been used for both images, and it does not show the full brightness range of the discrete sources. In the raw image, light (positive) spots are discrete sources in the *lead* field, while dark (negative) spots are discrete sources in the *trail* field. The brightest source in this image has a flux density of about 67 mJy at 31 GHz. These images were made from the entire dataset using natural weighting, have been corrected for the primary beam response, and have a resolution (FWHM) of $5\farcm2$–$5\farcm5$ (the resolution varies slightly across the image, depending on the u, v coverage obtained for each pointing).

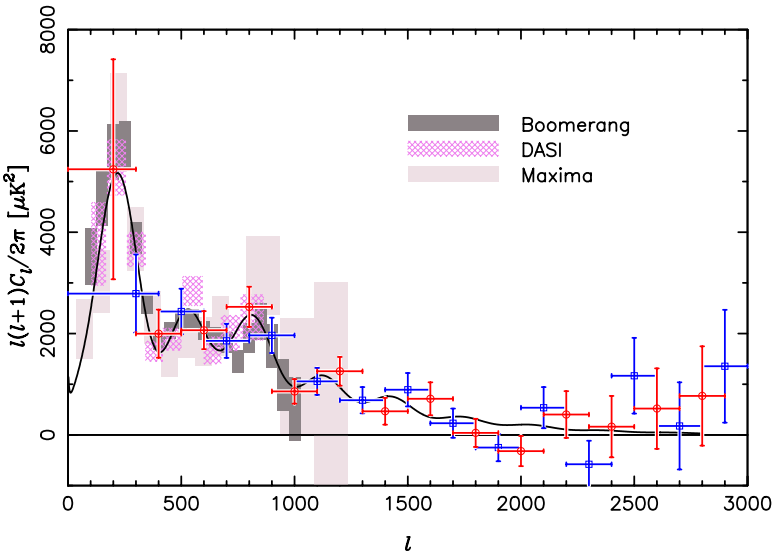

Fig. 2.— Comparison of the joint power spectrum estimates from the three CBI mosaic fields with the measurements from Boomerang (Netterfield et al. 2002), DASI (Halverson et al. 2002), and Maxima (Lee et al. 2001); the rectangles indicate the 68% confidence intervals on band-power. CBI band-power estimates have been made for two overlapping, *non-independent* divisions of the l range into bins (*blue squares and red circles*). The error-bars shows $\pm1\sigma$ uncertainties from the inverse Fisher matrix. The smooth curve is a cosmological model fitted to the CBI and earlier data (see Paper V).

We include constraint matrices (Bond, Jaffe, & Knox 1998) to project out the contributions of point sources of known position, and include a residual contribution from faint sources of unknown position. As an example, we show in Figure 2 the band-powers estimated from mosaic observations of three fields with bins of width $\Delta l = 200$; the correlation between adjacent bins is about -16% (see Paper III). We compare our results with the earlier results from the Boomerang, DASI, and Maxima experiments. In the region of overlap ($300 \lesssim l \lesssim 1000$) the agreement is very good. These results confirm the drop in power with increasing l first reported in Paper I, and extend the observations of this decline in power out to $l \sim 2000$, consistent with the extrapolation of models fitted to the low-l data; they provide improved constraints on cosmological parameters (see Paper V). At larger multipoles, $l = 2000$–3500, our deep observations (Paper II) are more sensitive, and they find that the power is 2.8σ greater than standard models for primary CMB anisotropy in this multipole range. This excess power is not consistent with expected levels of residual radio source contamination and is higher than predicted by most models of secondary anisotropy. If it is real, it could be due to secondary anisotropy generated by the Sunyaev-Zeldovich effect.

We gratefully acknowledge the generous support of Maxine and Ronald Linde, Cecil and Sally Drinkward, Barbara and Stanley Rawn, Jr., and Fred Kavli, and the strong support of the Provost and President of the California Institute of Technology, the PMA Division Chairman, the Director of the Owens Valley Radio Observatory, and our colleagues in the PMA Division. This work was supported by the National Science Foundation under grants AST 94-13935, AST 98-02989, and AST 00-98734. The computing facilities at CITA were funded by the Canada Foundation for Innovation. LB and JM acknowledge support by FONDECYT Grant 1010431. SC acknowledges support by CONICYT postdoctoral grant 3010037. We thank CONICYT for granting permission to operate within the Chanjnantor Scientific Preserve in Chile.

REFERENCES

Bond, J. R. & Efstathiou, G. 1987, MNRAS, 226, 655
Bond, J. R., Jaffe, A. H., & Knox, L. 1998, Phys. Rev. D, 57, 2117
Bond, J. R., et al. 2002, in preparation (Paper VI)
De Bernardis, P., et al. 2000, Nature, 404, 955
Halverson, N. W., et al. 2002, ApJ, 568, 38
Hanany, S., et al. 2000, ApJ, 545, L5
Hobson, M. P., Lasenby, A. N., & Jones, M. E. 1995, MNRAS, 275, 863
Hobson, M. P., & Maisinger, K. 2002, preprint (astro-ph/0201438)
Hu, W. & White, M. 1996, ApJ, 471, 30
Kamionkowski, M., & Kosowsky, A. 1999, Annu. Rev. Nucl. Part. Sci. 49, 77
Lee, A. T. et al. 2001, ApJ, 561, L1
Maisinger, K., Hobson, M. P., & Lasenby, A. N. 1997, MNRAS, 290, 313
Mason, B. S., et al. 2002, ApJ, submitted (Paper II)
Miller, A. D., et al. 1999 ApJ, 524, L1
Myers, S. T. et al. 2002, ApJ, submitted (Paper IV)
Netterfield, C. B., et al. 2002, ApJ, in press (preprint astro-ph/0104460)
Padin, S., Cartwright, J. K., Joy, M., & Meitzler, J. C., 2000, IEEE Trans. Antennas Propagat., 48, 836
Padin, S., et al. 2001, ApJ, 549, L1 (Paper I)
Padin, S., et al. 2002, PASP, 114, 83
Pearson, T. J., et al. 2002, ApJ, submitted (Paper III)
Sievers, J. L. et al. 2002, in preparation (Paper V)
Silk, J. 1968, ApJ, 151, 459
Sunyaev, R. A. & Zeldovich, Ya. B. 1970, Ap&SS, 7, 3
Sunyaev, R. A. & Zel'dovich, Y. B. 1972, ApJ, 4, 173
White, M., Carlstrom, J. E., Dragovan, M., & Holzapfel, W. L. 1999a, ApJ, 514, 12
White, M., Carlstrom, J. E., Dragovan, M., & Holzapfel, S. W. L. 1999b, preprint (astro-ph/9912422)
White, M., Scott, D., & Silk, J. 1994, Ann. Rev. A. & A., 32, 319